Developing fiber lasers with Bragg reflectors as deep sea hydrophones

Nicolò Beverini ([1])([3]), **Riccardo Falciai** ([2]), **Enrico Maccioni** ([1])([3]), **Mauro Morganti** ([1])([3]), **Fiodor Sorrentino** ([1]) **and Cosimo Trono** ([1])([2])

([1]) *Dipartimento di Fisica «E. Fermi», Università degli Studi di Pisa, Italy*

([2]) *Istituto di Fisica Applicata «Nello Carrara» (IFAC), CNR, Firenze, Italy*

([3]) *Istituto Nazionale di Fisica Nucleare (INFN), Sezione di Pisa, Italy*

Abstract

The present paper will discuss the work in progress at the Department of Physics of the University of Pisa in collaboration with the IFAC laboratory of CNR in Florence to develop pressure sensors with outstanding sensitivity in the acoustic and ultrasonic ranges. These devices are based on optically-pumped fiber lasers, where the mirrors are Bragg gratings written into the fiber core.

Key words *hydrophones – Bragg fiber-laser – pressure sensors*

1. Introduction

In the field of acoustic detection, piezoelectric sensors are the most widely used devices. This well established technology offers high reliability and relatively low cost production. Sensors based on optical fibers have well known advantages over conventional electro-mechanical sensors. They offer electrically passive operation and immunity from electromagnetic fields, since the fiber is realized entirely with dielectric materials (glass and plastic). They have very small dimensions (outer diameter ~125 μm for a standard fiber), and have multiplexing capabilities for a *quasi*-distributed measurement configuration, by using a single opto-electronic control unit. Remote measurement is also possible. Indeed, the very low signal attenuation (~0.3 dB/km) of the fibers in the region around 1.55 μm makes it possible to place the opto-electronic control unit several km far from the measurement point. Moreover, high sensitivity and wide dynamic measurement range can usually be achieved.

2. Fiber Bragg Grating sensors

A Fiber Bragg Grating (FBG) consists of a periodic perturbation of the optical fiber core refractive index. This grating acts on the radiation traveling in the fiber as a wavelength selective mirror. If the grating pitch is Λ, the reflection band is peaked at a wavelength

$$\lambda_{\text{Bragg}} = 2n_{\text{eff}}\Lambda \qquad (2.1)$$

where λ_{Bragg} is the so-called Bragg wavelength and n_{eff} is the effective refractive index. The width of the reflection band can be regulated by controlling the reflectivity of the mirror, that is by controlling the length of the grating (its total number of lines) and the depth of the reflection index modulation. Typical reflection bandwidth values are around 0.2 nm. Radiation outside the Bragg resonance condition will propagate in the fiber without perturbations (fig. 1).

Mailing address: Dr. Nicolò Beverini, Dipartimento di Fisica «E. Fermi», Università degli Studi di Pisa, Largo Pontecorvo 3, 56127 Pisa, Italy; e-mail: beverini@df.unipi.it

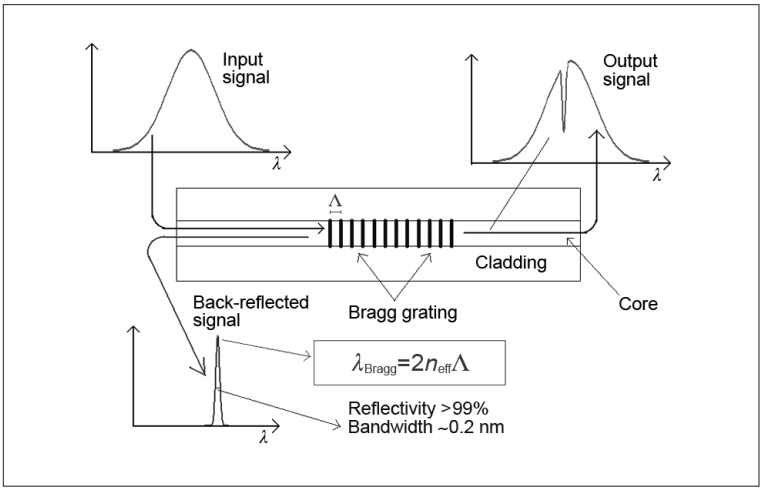

Fig. 1. Fiber Bragg grating reflection and transmission properties.

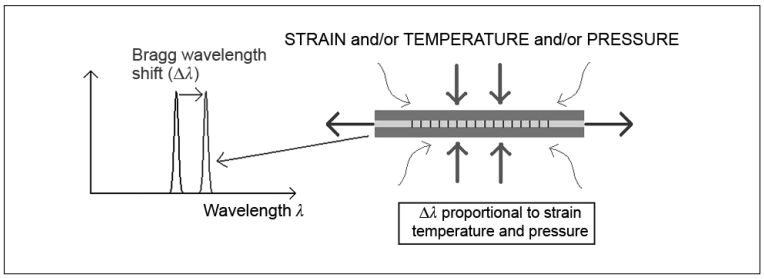

Fig. 2. Strain, temperature and pressure effects on a Bragg grating reflection spectrum.

FBGs are fabricated using the phase-mask technique on special Ge-doped fibers (Hill and Meltz, 1997). A phase-mask is a diffractive optical element which spatially modulates the UV writing beam (typically at $\lambda = 248$ nm, where the photosensitivity of the fiber is at its best). The near-field fringe pattern, which is produced behind the mask, photo-imprints a refractive index modulation on the core of the photosensitive fiber.

These gratings are highly sensitive to external perturbations that affect the fiber. With regard to eq. (2.1), every strain and temperature or pressure variation on the fiber changes both the grating pitch and the refractive index, producing a shift in the Bragg wavelength (fig. 2). The information is encoded on the wavelength, with the considerable advantage that a number of different gratings, with different Bragg wavelengths, can be inscribed on the same fiber and interrogated by the same opto-electronic unit, thus enabling a *quasi*-distributed measurement. The typical sensitivities of a fiber Bragg grating to strain, temperature, and pressure (which acts as an isotropic strain) are

$$\text{strain: } \frac{\Delta\lambda_{\text{Bragg}}}{\lambda_{\text{Bragg}}} = \left\{1 - \frac{n_{\text{eff}}^2}{2}\left[p_{12} - \nu(p_{11} - p_{12})\right]\right\}\varepsilon \tag{2.2}$$

temperature: $$\frac{\Delta\lambda_{\text{Bragg}}}{\lambda_{\text{Bragg}}} = (\alpha_\Lambda + \alpha_\nu)\Delta T \tag{2.3}$$

pressure: $$\frac{\Delta\lambda_{\text{Bragg}}}{\lambda_{\text{Bragg}}} = \left[-\frac{(1-2\nu)}{E} + \frac{n^2}{2E}(1-2\nu)\cdot (2p_{12}+p_{11})\right]\Delta P \tag{2.4}$$

where n_{eff} is the fiber effective refractive index, ν is Poisson's ratio, $\varepsilon=\Delta L/L$ is the strain (Bragg grating length L), p_{ij} are Pockel's coefficients of the stress-optic tensor, α_Λ is the thermal expansion coefficient, α_n represents the thermo-optic coefficient, and E is Young's modulus. For silica fibers, at 1550 nm the strain sensitivity is ~1.2 pm/$\mu\varepsilon$, the temperature sensitivity is ~10 pm/°C, and the pressure sensitivity is ~ −3.6 pm/MPa.

A typical FBG sensor device includes a broad-spectrum source (*i.e.* a superluminescent LED with ~ 40 nm spectral emission width). Its radiation is coupled into the fiber, and interacts with the grating. The wavelength shift of the reflection peak is then detected by means of spectro-photometric methods.

FBGs sensors are robust, can have a wide dynamic range, and can be easily multiplexed in order to realize multipoint detection at a low cost. Their ultimate sensitivity is limited, however, by the spectral bandwidth of the Bragg grating which at best can be of the order of 0.2 nm.

A typical application for FBG sensors is the control of deformations in structures to which the gratings can be attached or within which they can be embedded. The following is a summary of FBG sensor applications made by the IFAC group:

– Applications for the cultural heritage (Castelli *et al.*, 2003): *in situ* measurement and continuous monitoring of deformations in painted wood panels.

– Automotive applications: monitoring of deformations in car windshields (Falciai *et al.*, 2004).

– Structural health monitoring: FBGs embedded in carbon fibers in composite strips for concrete beam reinforcement and monitoring (Falciai *et al.*, 2005).

FBGs show only a limited responsivity to variations in pressure (the typical wavelength resolution of FBG interrogation systems is ~1 pm, which means approximately 0.3 MPa, or 3 atm). Therefore, their typical application is for high pressure sensing (Xu *et al.*,1993).

3. Fiber lasers

A Distributed Bragg Reflector Fiber Laser (DBR-FL) consists of two Bragg gratings with identical reflection wavelengths (Ball and Glenn, 1992), which are directly inscribed in a single-mode erbium-doped optical fiber (fig. 3). When pumped with 980 nm radiation, this structure acts as an active medium inserted in a Fabry-Perot laser cavity, with an emission peak around 1530 nm. The power emitted is a function of the broadband source pumping power, the length of the laser cavity and the Bragg gratings reflectivity,

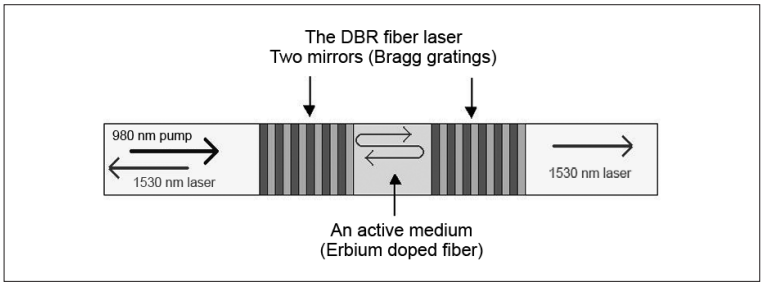

Fig. 3. Fiber laser pumping scheme.

but it is in any case some orders of magnitude higher than the power available on the reflected radiation from a passive FBG sensors. Cavity length is an important laser parameter. The emitted laser power increases with the cavity length, but a shorter length means a larger separation between the resonant longitudinal modes ($\lambda = \lambda^2/2L$). With a cavity length of a few cm, only one cavity mode lies inside the optical bandwidth of the Bragg gratings, and it becomes possible to operate with the laser in a stable single-frequency emission mode. In these conditions the laser line-width is very narrow (<5 kHz, equivalent to a coherence length of over 30 km). The comparison between the performances of devices using the FBG and the DBR is provided in table I.

The very narrow line-width means that the DBR laser sensor is intrinsically more sensitive than the FBG sensor; for this reason, it seems particularly suitable for very low-pressure measurements.

Table I. Comparison of FBG and DBR performances.

	Power	Line-width (kHz)	Line-width (nm)
FBG (passive)	1-100 nW	$\sim 10^7$	~0.1
DBR (active)	100 μW-1 mW	~5	$\sim 5 \cdot 10^{-8}$

DBR fiber lasers were fabricated in the IFAC laboratories. An excimer (KrF) UV laser, with emission at 248 nm, was used for Bragg gratings writing. We obtained a Bragg grating with $\lambda_{Bragg} \cong 1532$ nm by a phase mask with a nominal spatial period of 1059.9 nm on an erbium doped fiber having an absorption coefficient of 14 dB/m at 980 nm. The length of Bragg gratings was 1 cm, and we chose the distance between the two FBG reflectors and the FBGs reflectivity in order to obtain the maximum power emission in stable, single longitudinal mode regime. Typical values are: output FBG reflectivity: >90%; back FBG reflectivity: >99%; distance between the FBGs: 2 mm-2 cm; emission power: 10 μW-1 mW with about 200 mW of 980 nm pumping power.

The laser line-width was measured by heterodyning on a fast photodiode the beams from two different lasers with slightly different emission wavelengths, and then observing the resulting beat note on a radio-frequency spectrum analyzer. We could estimate a line-width narrower than 5 kHz.

It is possible to inscribe several laser structures on a single doped fiber with the aim of multiplexing a few sensors, by working at slightly different wavelengths on the same fiber with a common pump laser. In order to test multiplexing operation, we wrote two lasers on the same optical fiber with a different grating pitch. Figure 4

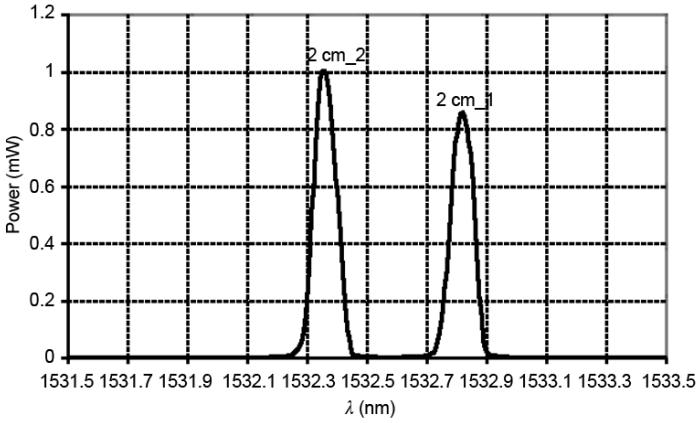

Fig. 4. Emission spectrum of an array of two fiber lasers.

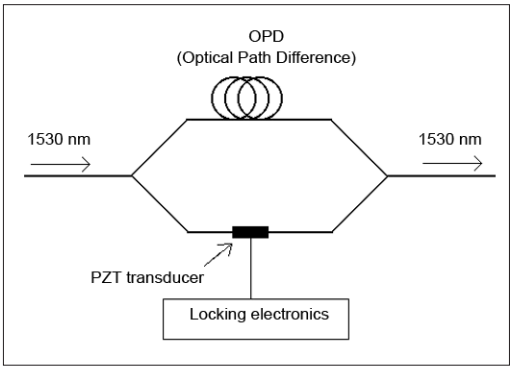

Fig. 5. The Mach-Zender Interferometer.

reports the emission spectrum of this two-laser array, acquired by means of an optical spectrum analyzer (wavelength resolution: 0.1 nm).

4. Fiber laser hydrophone

In developing highly sensitive hydrophones for deep sea applications, the ultimate goal is to achieve a sensitivity at the level of the acoustic background noise of the quiet ocean, which is conventionally represented by the so-called Deep Sea State Zero (DSS0) (Wenz, 1962). At 1 kHz, the DSS0 level is 100 μPa/Hz$^{1/2}$, which should correspond (eq. (2.4)) to a wavelength shift of approximately 10^{-12} nm, 11 orders of magnitude less than the typical FBG bandwidth. The DBR fiber laser emits monochromatic radiation with a line-width of approximately $4 \cdot 10^{-8}$ nm, and an interferometric detection technique provides the possibility of pushing the sensitivity a factor 10^3-10^4 below the laser line-width, thus approaching the sensitivity required by the DSS0 level. Figure 5 shows the scheme of an unbalanced Mach-Zender interferometer (MZI), which we used in our detection scheme.

The interferometer converts the pressure-induced wavelength shift of the radiation emitted by the DBR fiber laser into a phase delay. The phase difference $\Delta\varphi_{MZ}$ at the MZI output is dependent on the fiber laser output wavelength shift $\Delta\lambda$ and on the Optical Path Difference (OPD= $= nL$), which is the length difference L of the two interferometer arms times the fiber core refractive index n. The following relationship holds:

$$\Delta\varphi_{MZ} = \frac{2\pi \cdot \mathrm{OPD}}{\lambda^2}\Delta\lambda. \qquad (4.1)$$

With λ of the order of 10^{-12} nm (DSS0 conditions), an OPD of 300 m gives a value of $\varphi_{MZ} \approx 1$ μrad, which is a resolution achievable with the present technology (Kersey *et al.*, 1992).

5. Experimental tests

We made a preliminary characterization of the sensor in our laboratory and tested the responsivity of our lasers by using a MZI with OPDs of 150 m and 450 m. According to eq. (4.1), the MZI responsivity increases by increasing the unbalance, up to the limit given by the coherence length of the laser radiation, which for these lasers consists of many km. The monotonic operative range and the dynamic range are, however, reduced proportionally. Indeed, the phase detector signal is not univocally related to the wavelength shift, when the phase difference grows over 2π radians, and the low frequency noise of the laser exceeds this limit, yet with a few meter of length unbalance. We were then obliged to lock the MZI phase to the laser frequency at low Fourier frequencies, with a cut-off of the order of several kHz, by using a servo loop that acts on the length of one arm of the interferometer by stretching the fiber through a piezoelectric actuator. The interferometer was used in the condition usually defined as «quadrature» detection (Kersey *et al.*, 1992), with the MZI locked at one side of a fringe in the middle point, where the sinusoidal function is proportional to the phase and the responsivity has its maximum value.

The experimental apparatus is sketched in fig. 6. The fiber laser was sink in a 1 m^3 water tank, close to a conventional Piezo-Transducer (PZT) hydrophone for calibration and validation; a SDR HS/150 model was used with a nominal responsivity of 1.778 mV/Pa (29 dB

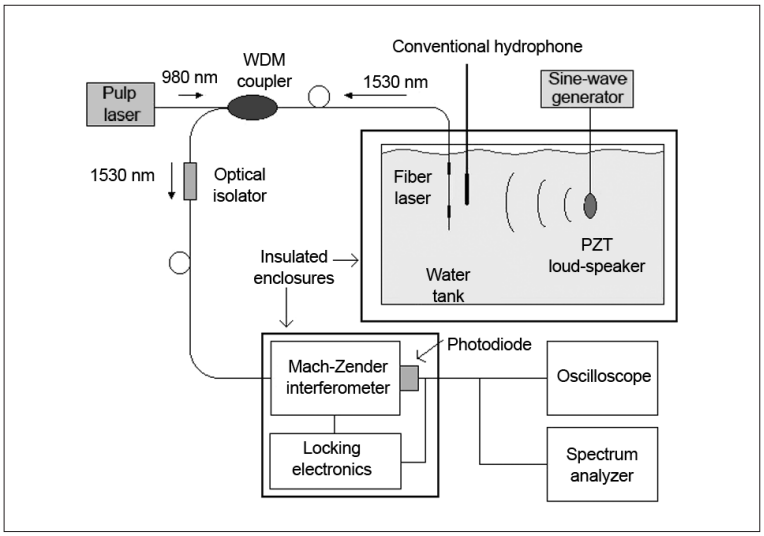

Fig. 6. Experimental setup.

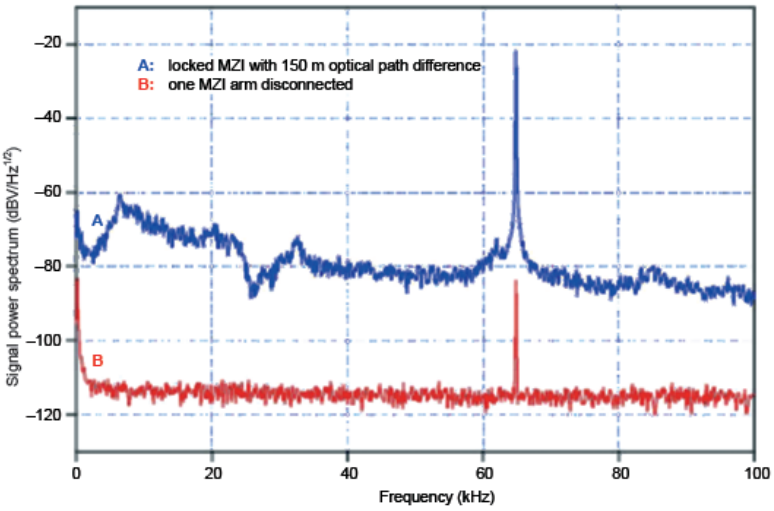

Fig. 7. Fiber laser spectral response to a 65 KHz test tone (OPD = 150 m). *Top* (A): the fiber laser response (output of the MZI) to a 65 kHz loud-speaker acoustic test note. *Bottom* (B): the laser output spectrum (without the MZI).

amplification). A PZT loud-speaker provided a cw sinusoidal uncalibrated acoustic signal. The laser emission wavelength modulation, induced by the acoustic signal, was converted into phase modulation by the Mach-Zender interferometer, and analyzed by means of an electronic spectrum analyzer (125 Hz resolution bandwidth).

Figure 7 compares the MZI output with the laser output spectrum in the absence of the interferometer when the fiber laser was stimulated with a 65 kHz acoustic wave. From these two spectra we deduced a limit for the performance of a particular FL sensor, referred to a device of a specific optical power (100 μW), and a fixed orientation with respect to the acoustic source. In fact the upper base line –80 dBV/Hz$^{1/2}$ level, corresponding to about 56 mPa/Hz$^{1/2}$, was produced by the actual environmental noise level. The bottom –118 dBV/Hz$^{1/2}$ level, which corresponds to about 0.7 mPa/Hz$^{1/2}$, represented the opto-electronic noise level, and thus the lowest

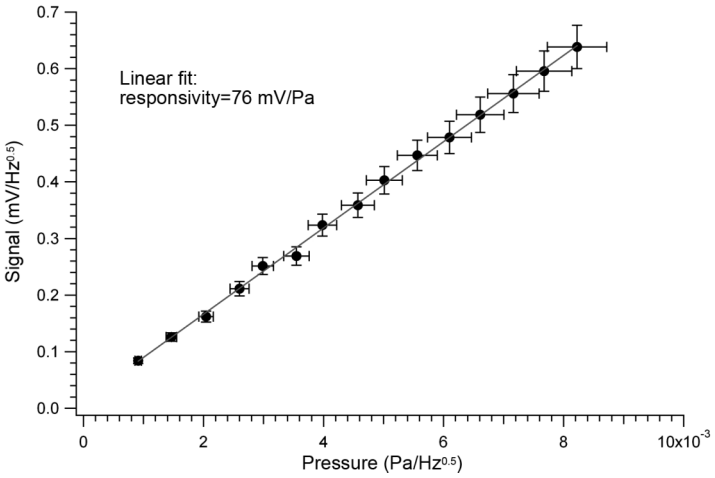

Fig. 8. FL output signal *versus* pressure (measured with the calibrated reference hydrophone). FL optical power 10 μW, test note frequency 40 kHz; OPD ~450 m. Error bars represent the reading uncertainty.

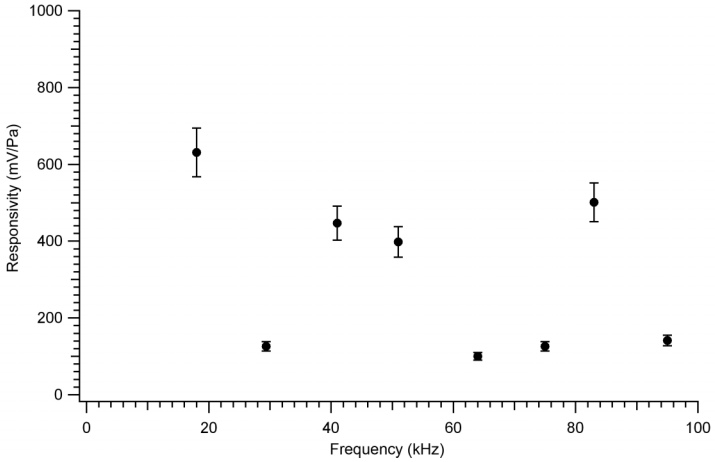

Fig. 9. FL responsivity for different test note frequencies; OPD ~ 450m; FL optical power 10 μW.

attainable limit for the minimum detectable signal of the fiber laser. The acoustic level in mPa was estimated by means of a comparison with the readings of a calibrated PZT hydrophone.

We measured the response of the device to in-water acoustic notes at several fixed frequencies in the region between about 15 and 100 kHz, for different intensities of loud-speaker excitation. By making a comparison with the calibrated PZT hydrophone, we observed a highly linear trend of the FL output signal *versus* pressure (fig. 8). In this particular experimental condition, we measured a responsivity of 76 mV/Pa at 40 kHz, where the voltage value refers to the photodiode signal at the MZI output. The reading error bars (± 0.5 db) on the single measurement are reported.

However, the responsivity is changing significantly as a function of the acoustic wave frequency. Figure 9 reports measured responsivities for a same FL and a same Mach-Zender OPD. The large spread for the responsivity values depends strongly on the particular set of experimental parameters. In fact, it can be affected at some specific frequencies by the acoustic reflections between the walls of the water tank, due to its reduced dimensions. Also mechanical resonances of the fiber laser holder, and of the fiber itself, may have caused a dependence of the frequency response. Moreover, the acoustic perturbation in water may act differently on the two Bragg gratings of the laser, because they are spatially separated. All these factors dictate that a true characterization of the sensors should be made only under better control of experimental conditions, operating in a large pool and in pulsed excitation regime, in order to avoid reflection effects. In particular, it will be important to study the dependence of the response on the orientation of the sensor. In any case, we can say that the pressure dynamic range for the FL sensor set-up shown in figs. 8 and 9 is roughly of four decades. In fact, the minimum detectable pressure in this experimental condition is of the order of 1 mPa/ $Hz^{1/2}$ at every frequency; this is, for example, the measured value of the first point on fig. 8. The output voltage of the device is linear with pressure up to about 1 V, that is, up to 10 Pa with minimum responsivity in the 15-100 kHz range of approximately 100 mV/Pa (fig. 9).

6. Conclusions

The results of the study, development and experimental validation of a DBR fiber laser for acoustic sensing in marine environment, have been reported. Single mode lasers were fabricated by writing two Bragg gratings on an erbium-doped fiber core. The very narrow linewidth (<5 kHz), combined with an interferometric detection, could make possible a wavelength resolution of $\sim 10^{-12}$ nm. The comparison with a calibrated PZT hydrophone (15-100 kHz frequency range) showed a highly linear trend of the fiber laser output signal *versus* pressure. On the other hand, FL responsivity was strongly frequency dependent. This fact was probably connected to the particular experimental set-up, such as the acoustic reflections between the walls of the water tank and the mechanical resonance of the FL holder and of the fiber itself.

The FBG hydrophones offer a wide range of applications, ranging from the marine environmental acoustic monitoring to the deep-sea study and the survey of dolphins and whales. In general, a network of multiplexed FBG hydrophones could provide much information on what happens in the «under-the-sea world» in the acoustic and ultrasound regimes, whichever could be the origin of the propagating pressure wave. An interesting field of application could be the acoustic detection of particle showers produced in water by very high-energy neutrinos, as an alternative method to the more conventional photo-detection.

Acknowledgements

This research was supported by the Italian University Ministry (MIUR), by the University of Pisa, by National Institute of Nuclear Physics (INFN), and by the Italian National Research Council (CNR).

REFERENCES

BALL, G.A. and W.H. GLENN (1992): Design of a single-mode linear-cavity erbium fiber laser utilizing Bragg reflectors, *J. Lightwave Tech.*, **10**, 1338-1343.

CASTELLI, C., G. LANTERNA, R. FALCIAI and C. TRONO

(2003): Continuous monitoring of wooden works of art using fiber Bragg-grating sensors, *J. Cultural Heritage*, **4**, 285-290.

FALCIAI, R., C. TRONO, P. CASTELLI, R. GALLI, N. MATTIUCCI and N. PALLARO (2004): Automotive applications of fiber Bragg grating sensors, in *Proceedings of the 8th Conference Sensors and Microsystems «Aisem 2003»*, edited by C. DI NATALE, A. D'AMICO, G. SONCINI, L. FERRARIO and M. ZEN (World Scientific Publisher), p. 545.

FALCIAI, R., J.M. KENNY, A. TERENZI, C. TRONO and R. MEZZACASA (2005): Reinforcing and monitoring of concrete structures with composites and fiber optic sensors, in *Proceedings of the 9th Conference Sensors and Microsystems «Aisem 2004»*, edited by C. DI NATALE, A. D'AMICO, G. MARTINELLI, M.C. CAROTTA and V. GUIDI (World Scientific Publisher), 329-336

HILL, K.O. and G. MELTZ (1997): Fiber Bragg Grating technology fundamentals and overview, *J. Lightwave Technol.*, **15** (8), 1263

KERSEY, A.D., T.A. BERKOFF and W.W. MOREY (1992): High-resolution fibre-grating based strain sensor with interferometric wavelength-shift detection, *Electron. Lett.*, **28** (3), 236-238.

WENZ, G.M. (1962): Acoustic ambient noise in the ocean: spectra and sources, *J. Acoust. Soc. Am.*, **34**, 1936-1956.

XU, M.G., L. REEKIE, Y.T. CHOW and J.P. DAKIN (1993): Optical in-fibre grating high pressure sensor, *Electron. Lett.*, **29**, 398-399.

(received September 6, 2005;
accepted May 17, 2006)